Sterically Crowded Tris(2-(trimethylsilyl)phenyl)phosphine – Is it Still a Ligand?

Hans Gildenast,[a] Felix Garg,[a] and Ulli Englert*[a, b]

Dedicated to Professor Holger Braunschweig at the occasion of his 60th birthday.

Abstract: Tris(2-(trimethylsilyl)phenyl)phosphine, P(o-TMSC$_6$H$_4$)$_3$, was synthesised and characterised in solution and in the solid state. The large steric bulk prevents most reactions of the phosphorus donor and makes the compound air stable both in the solid state as well as in solution. This shielded phosphine can still undergo three reactions, namely protonation, oxidation to the phosphine oxide under harsh conditions and complexation to Au^I, thus forming a complex with linear coordination. Unexpectedly, complexation was unsuccessful with a range of other metal cations. Neither Pd^{II}, Pt^{II}, Zn^{II} nor Hg^{II} reacted and even the remaining coinage metal cations Cu^I and Ag^I could not be coordinated. Both the parent molecule as well as the reaction products were structurally characterised by single crystal X-ray diffraction, and the conformational change of geometry required to accommodate the additional atoms was analysed in detail. Apart from chemical oxidation with H$_2$O$_2$, P(o-TMSC$_6$H$_4$)$_3$ displays reversible electrochemical oxidation with a potential not unlike the one of sterically unencumbered phosphines for which the oxidation is usually not reversible. P(o-TMSC$_6$H$_4$)$_3$ can thus be considered a model compound for the investigation of the electronic properties of sterically unencumbered phosphines.

Introduction

Early research on phosphines and especially their tertiary derivatives and transition metal complexes dates back to the 19th century, and today phosphines have a fixed place in modern coordination chemistry.[1–4] The property of phosphorus as a soft donor atom according to Pearson allows it to stabilise metals in low oxidation states.[5–8] The large scale industrial processes employing phosphines as ligands are dominated by the simple and inexpensive ones such as PPh$_3$ and its sulphonated derivatives. Besides their use in hydroformylation[9,10] a range of multi-ton processes incorporates phosphines to stabilise transition metals.[11] On smaller scale syntheses a wide range of tailored phosphines is used as ligands in a variety of reactions ranging from asymmetric hydrogenation to cross coupling reactions.[12–15] The activity, selectivity and stability of the catalyst complexes is dictated by both the electronic structure of the phosphine as well as the steric demand and repulsion exerted onto the substrate.[16–20]

PCy$_3$ for example is an excellent ligand in Sonogashira coupling reactions as the high steric demand of the cyclohexyl groups favours the formation of Pd^0 species with low coordination numbers facilitating oxidative addition.[21]

In numerous examples the steric bulk of the phosphine can be used to control regioselectivity of metal catalysed reactions.[22–24] The quantification of steric bulk was pioneered by C. Tolman who defined the ligand cone angle θ as a single descriptor for steric bulk.[25] A more recent approach is the buried volume V_{Bur}[26,27] which is defined as the percentage of a sphere around the metal centre that is occupied by a ligand. Moving away from single numerical descriptors it is now an established method to classify steric bulk with topographic maps.[28,29] Obviously, the steric bulk can only be increased up to a certain extent without completely preventing metal coordination. Beyond that limit, a different interaction between phosphine and metal cation can be observed.[30] Sterically overcrowded phosphines such as P(Mes)$_3$ and P(2,6-iPrC$_6$H$_3$)$_3$ have been oxidized both electrochemically or by Ag^I cations yielding radical cations sufficiently stable to be investigated spectroscopically and more recently even with diffraction methods.[31–33]

In the course of our research we encountered the sterically crowded phosphine tris(2-(trimethylsilyl)phenyl)phosphine (P(o-TMSC$_6$H$_4$)$_3$, **2**, Figure 1). The three trimethylsilyl (TMS) groups generate a large steric bulk shielding the phosphorus. The distribution of steric bulk on a single side of each ring sets it

[a] H. Gildenast, F. Garg, Prof. Dr. U. Englert
RWTH Aachen University,
Institute of Inorganic Chemistry,
Aachen, Germany
E-mail: ullrich.englert@ac.rwth-aachen.de

[b] Prof. Dr. U. Englert
Shanxi University,
Key Laboratory of Materials for Energy Conversion and Storage,
Institute of Molecular Science, Taiyuan,
Shanxi 030006, People's Republic of China

Chemistry–A European Journal

Full Paper
doi.org/10.1002/chem.202103555

Chemistry Europe
European Chemical
Societies Publishing
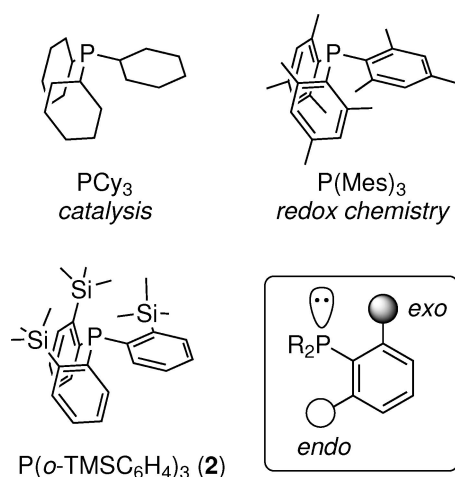
Figure 1. Two prototypic sterically crowded phosphines and our compound P(o-TMSC₆H₄)₃ (**2**). PCy₃ is used in numerous laboratory scale catalyses and P(Mes)₃ is able to form rather stable radical cations. The box shows the *exo* and *endo* nomenclature used to classify the conformation of *ortho* substituted arylphosphines.

apart from overcrowded phosphines such as P(Mes)₃ and P(2,6-iPrC₆H₃)₃ with substituents on both the *exo* and *endo* side (Figure 1).[34]

Compounds with similar single sided steric bulk have been prepared such as P(o-(CF₃)C₆H₄)₃ and P(o-(iPr)C₆H₄)₃. In their uncoordinated form these prefer the *exo₃* conformation in which all substituents reside on that side of the phosphine.[35,36] Nevertheless, both can adopt the *exo₂* conformation in which one substituent flips to the *endo* side. This reduces steric bulk on the *exo* side while increasing steric pressure on the *endo* side.[37] The realisation of this compromise is seen upon coordination as the additional atoms attached to the phosphine increase steric pressure on the *exo* side.[38,39] The mechanism and kinetics of the ring flips necessary to transform from *exo₃* to *exo₂* has been investigated thoroughly both experimentally and with theoretical methods.[40] A direct comparison for our ligand would be a triarylphosphine bearing three *ortho* t-butyl groups which to the best of our knowledge has not been reported so far. So we were curious to find out whether our phosphine **2** is inert enough to form a stable radical cation and if it is indeed still a ligand?

Results and Discussion

The compound tris(2-(trimethylsilyl)phenyl)phosphine (P(o-TMSC₆H₄)₃, **2**) is accessible *via* the path shown in Figure 2.

Tris(2-bromophenyl)phosphine (**1**) is subjected to a triple bromine lithium exchange and subsequently reacted with trimethylsilylchloride (TMSCl) to afford **2**. If TMSCl is used in excess, **2** is the main product of this reaction but not the only one. A side reaction gives compound **3**. We suspected a contamination of the TMSCl with dimethylsilyldichloride, but found no trace of the latter in the material used. Consequently the reaction to **3** requires an abstraction of a methyl group
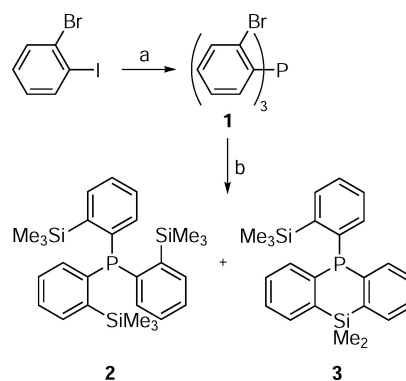
Figure 2. Synthesis scheme for **2** and the side product **3**. (a) 1. *i*-PrMgCl 2. PCl₃, CuI. (b) 1. *t*-BuLi 2. TMSCl.

from the TMS moiety. This may be mediated by another TMSCl molecule as shown in the proposed mechanism in Figure 3 as the abstraction of a CH₃⁻ anion seems irrational.

The identity of **3** was confirmed by spectroscopy and diffraction methods. The crystal structures of this dimorphic by-product are discussed in the Supporting Information. The extent of this side reaction can be suppressed to about 25% by using TMSCl in large excess.

Structural features of 2

Compound **2** crystallises in the trigonal space group $R\bar{3}$ with $Z = 12$. The structure features two symmetry independent molecules **A** and **B** (Figure 4) both in *exo₃* conformation.
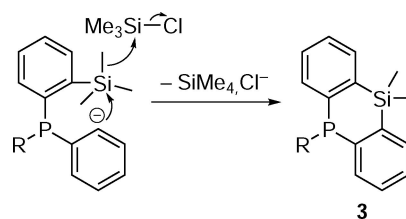
Figure 3. Proposed mechanism for the formation of **3**.
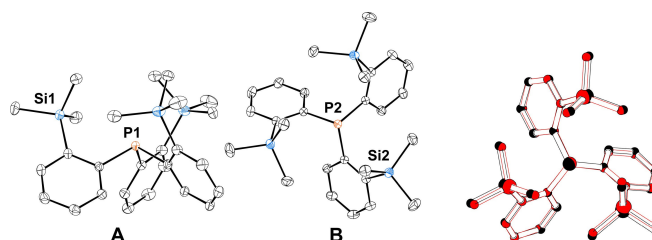
Figure 4. Displacement ellipsoid plot of **2**. The two symmetry independent molecules **A** and **B** are displayed from two different perspectives and not in their correct relative orientations in the packing. On the right the overlay of **A** (red) and **B** (black) is shown.

Chemistry–A European Journal

Full Paper
doi.org/10.1002/chem.202103555

Chemistry
Europe
European Chemical
Societies Publishing

The P atoms of both molecules are situated on the crystallographic threefold axis, with only one third of each molecule being symmetrically independent. To obtain an accurate picture of the geometry of **2** we collected high resolution diffraction data up to a resolution of 0.45 Å (1.11 Å^{-1}). Relevant geometrical parameters for **2** and four phosphines from literature for comparison are listed in Table 1. We also conducted a database research to compare the geometry of **2** to triarylphosphines in general and sorted them according to the number and position of their *ortho* substituents (Figure 5).

This shows that the C–P–C angle is particularly sensitive towards steric *endo* pressure caused by the presence of 2,6-substituted rings. The number of single sided substituents appears to have little influence on this angle and only a slight trend towards lower angles caused by *exo* substituent repulsion occurs. The C–P bond distance appears to be loosely correlated to the number of *otho* substituents and elongate with higher substitution. Overall **2** displays a geometry not uncommon for a phosphine with its substitution pattern despite the large sterical demand of the TMS groups.

In return the little change in the C–P–C bond angles with respect to sterically unencumbered phosphines intuitively suggests that the TMS groups should come very close to each other. This does not appear to be the case either. The shortest H···H distances between the three TMS groups are all above 2.45 Å which is well outside the sum of the van der Waals radii of two hydrogen atoms.[44] The TMS groups furthermore dictate the tilt of the phenyl rings with respect to the axis of the phosphorus and its lone pair ω (Figure 6).

A low ω tilt would lead to collision between the TMS groups above the phosphine while a flattening of the triaryl propeller will lead to collision between the TMS groups with their neighbouring compared to the phenyl rings. Incidently, with an average of 41(3)° the ω tilt for **2** is larger by less than 5° compared to the average ω tilt of plain PPh$_3$.[41] However, the three individual ω tilts in PPh$_3$ deviate strongly from each other owing to their conformational freedom. Overall, the TMS groups in **2** sterically shield the phosphorus atom from most external influences without generating significant steric pressure. This allows the molecule to retain the static geometry of a phosphine without *ortho* position substituents while forfeiting the dynamic freedom.

The trigonal packing features no directional short intermolecular contacts due to the non-polar nature of this compound. There are, however, distinct interlocks between the molecules (Figure 7). **A** engages in a sextuple phenyl embrace with its symmetry equivalent generated by the $\bar{3}$ rotoinversion at Wyckoff position 3*b*.[45] The two units of **B** located around the $\bar{3}$

Table 1. Comparison of geometrical parameters for the description of our compound **2** and other tiarylphosphines.[35,40,42,65]

	C–P/Å	C–P–C	ω/
P(o-TMSC$_6$H$_4$)$_3$ (**2**)	1.8443(7)	102.27(13)	41(3)
P(CF$_3$C$_6$H$_4$)$_3$	1.843(11)	101.4(5)	36.9(19)
P(o-iPr$_6$H$_4$)$_3$	1.837(4)	102.3(11)	43(7)
PMes$_3$	1.837(4)	109.7(13)	44(5)
PPh$_3$	1.830(3)	102.7(10)	37(19)

All values are the averages of equivalent parameters within the same structure. Numbers in parentheses are standard deviations of the averaged values and do not correspond to errors from the structure determination.
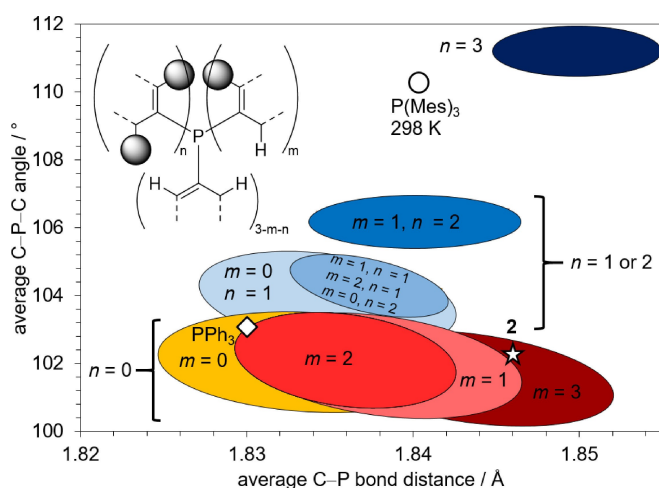
Figure 5. Scatter plot of C–P distances versus C–P–C angles for triarylphosphines in the CSD.[43] Individual data points have been clustered with respect to distribution and number of non-hydrogen substituents in *ortho* position and represented by coloured ellipses. Coloured yellow are phosphines without *ortho* substituents ($n=0$ and $m=0$). Coloured red are phosphines where no rings have two *ortho* substituents ($n=0$). Darker reds indicate a greater number of rings with one *ortho* substituent. Coloured blue are phosphines where at least one ring has two *ortho* substituents ($n\geq 1$). The data for PPh$_3$, P(Mes)$_3$ and **2** have been marked as a diamond, circle and a star respectively. Error-free datasets collected at T≤200 K with R ≤0.05; polymers and disordered structures have been excluded. Additional information about the data is given in the Supporting Information.

Figure 6. Chemical diagram and Newman plot defining the geometrical parameter ω. The direction of view is through the P–C bond and the bold line in the background represents one phenyl ring. The remaining two are not depicted in the Newman plot for clarity.
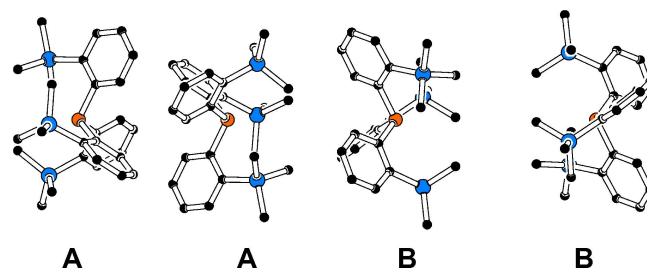
Figure 7. Packing of **2** along *b* displaying the alternating intermolecular interlocks of the molecules **A** and **B**.

Chemistry–A European Journal

Full Paper
doi.org/10.1002/chem.202103555

Chemistry Europe
European Chemical
Societies Publishing

rotoinversion 3a engage in a related interlock of their TMS groups with their symmetry equivalents. The interaction between **A** and **B** is the interlock of the TMS groups of **A** with the phenyl groups of **B**. These interactions arrange the molecules in (AABB)$_\infty$ stacks along *c*. Between the individual stacks there are no short contacts or prominent packing features.

Reactivity of 2

Looking at the space filling CPK model[46] of **2** (Figure 8), the phosphorus atom appears to be shielded well from external influences. However, the crystal structure cannot represent the conformational freedom **2** may have in solution. To test the inertness of **2** we attempted reactions common for triarylphosphines (Table 2).

The smallest possible reactant for a phosphine is a proton as phosphines can act as bases. We performed an experiment in analogy to the study on the basicity of phosphines by T. Allman
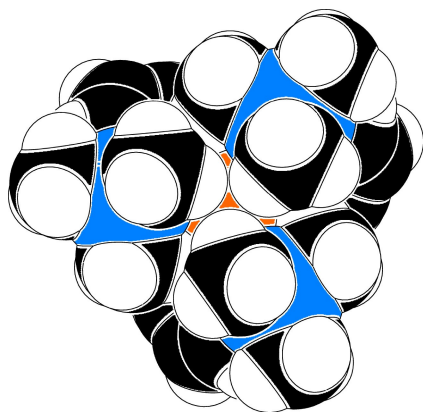
Figure 8. Space filling plot of the symmetry independent molecule **A** in the crystal structure of **2**; Si atoms are shown in blue, P in orange.

Table 2. Summary of the reactions attempted with **2**. a: Lawesson's reagent.
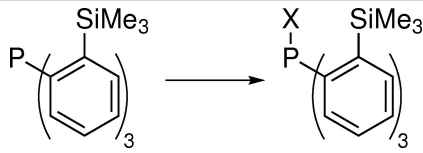
reactant	X
CF$_3$COOH	H$^+$
HClO$_4$	H$^+$ (**4**)
BH$_3$	–
B(C$_6$F$_5$)$_3$, H$_2$	–
[PdCl$_2$(MeCN)$_2$]	–
[PtCl$_2$(COD)]	–
[Cu(MeCN)$_4$]ClO$_4$	–
CuCl	–
[AuCl(tht)]	AuCl (**5**)
AgPF$_6$	–
Zn(OTf)$_2$	–
H$_2$O$_2$/mCPBA	O^{2-} (**6**)
S$_8$/LR^a	–

and R. G. Goel by measuring NMR spectra of **2** in trifluoroacetic acid.[47] Both the ^{1}H and ^{31}P spectra display the expected $^1J_{P-H}$ coupling with a coupling constant of 484 Hz which is smaller by 20 Hz than for PPh$_3$ (504 Hz), similar to that of P(*o*-Tol)$_3$ (491 Hz) and in total not surprising for a triarylphosphine. The reaction with the strong inorganic acid HClO$_4$ gave the protonated species which could be confirmed by single crystal analysis of [HP(*o*-TMSC$_6$H$_4$)$_3$]ClO$_4$ (**4**). Both experiments confirm that the weakly basic property of **2** is not impeded.

This behaviour – possible protonation but next to no reactions with larger Lewis acids – is reminiscent of the sterically hindered base 2,6-di-*t*-butylpyridine.[48] Accordingly, **2** shows no reactivity towards larger non-metal Lewis acids such as BH$_3$. Hydrogen activation with the potential frustrated Lewis pair of **2** with B(C$_6$F$_5$)$_3$ was also unsuccessful.

The reactivity towards metal cations as Lewis acids is also nearly completely inhibited. Coordination to the metal cations listed in Table 2 was attempted and unsuccessful based on the absent shift of the ^{31}P NMR signal of the phosphorus. Surprisingly, the only successful coordination was observed with Au^I, one of the largest metal cations. The formation of [AuCl(P(*o*-TMSC$_6$H$_4$)$_3$)] (**5**) can be easily observed with ^{31}P NMR spectroscopy, takes about an entire day to complete at room temperature and is accompanied by the precipitation of Au^0. Most phosphines finish this reaction within seconds. We attribute this slow reaction rate to the considerable structural rearrangement the ligand has to undergo to fit the Au^I cation. This selectivity towards the largest of the coinage metal cations appears irrational with regard to the significant steric encumbrance of the coordination site. On the other hand, the M–P bond is the most stable for Au^I among the coinage metal cations as investigated by Schwerdtfeger and co-workers. They suggested that this is the result of the increase in electronegativity for gold due to relativistic effects[49] and that this in turn amplifies the susceptibility for σ-charge donation from the phosphine lone pair.[50] The lower stability of the Cu/Ag–P bonds may result in a complex formation constant too low to be observed for **2**.

Besides the reversible addition of Lewis acids and metal cations, phosphines can also undergo oxidation reactions with chalcogenes. While most triarylphosphines react slowly with ambient oxygen when dissolved and exposed to air, **2** appears to be indefinitely stable towards air. More harsh oxidating conditions such as the exposure to H$_2$O$_2$ or mCPBA can after all oxidise **2** giving the phosphine oxide OP(*o*-TMSC$_6$H$_4$)$_3$ (**6**). Addition of the heavier chalcogen sulphur was unsuccessful. The reaction with selenium was thus not attempted.

In summary, the restricted reactivity of **2** reflects the significant steric hindrance.

Structural features of the reaction products

The structural parameters of the reaction products reveal how the tightly closed environment around the P atom changes in a concerted manner to enable chemical interactions with this atom. Definitions of the angles and torsions required for this

Chemistry–A European Journal

Full Paper
doi.org/10.1002/chem.202103555

Chemistry Europe
European Chemical
Societies Publishing

discussion are shown in Figure 9 and their values are listed in Table 3. Comparisons between the structures of each reaction product and **2** are displayed in Figure 10. The sense of rotation
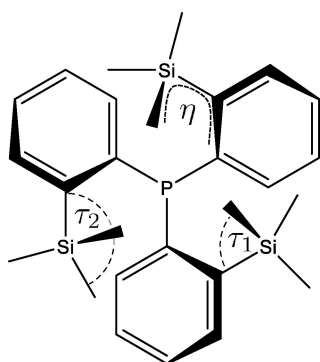
Figure 9. Chemical diagram of **2** defining the geometrical parameters. η is the torsion of the TMS group with respect to the adjacent phenyl ring. The CH_3 carbon used for this parameter is always the one pointing towards the centre of the molecule. τ_1 is the C–Si–C angle with the aforementioned CH_3 group while τ_2 is the angle formed with the CH_3 group pointing towards the neighbouring phenyl ring.

for the TMS groups has been chosen arbitrarily; inversion symmetry implies the concomitant presence of the opposite sense.

The crystal structure of the protonated species **4** displays a shortening of the P–C bonds corresponding to the more contracted electron density of phosphorus after protonation. Simultaneously the C–P–C angles become more obtuse. Both effects alone would contract the phosphine cavity even further. These conformational changes are compensated by an increase in the ω ring tilt of about 11° with a simultaneous 49° clockwise η rotation to avoid collision of a CH_3 group with the neighbouring phenyl ring. This is accompanied by a considerable increase of the 1,4 P⋯Si distance indicating a deformation of the aryl substituent angles and thus steric strain. The additional 5° increase in τ_1 emphasizes this steric strain generated by the acidic proton. Overall, these movements lead to an opening of the phosphine cavity placing the closest H⋯H distance of the TMS groups at 2.98 Å (2.45 Å for plain **2**) and each of them 2.32 Å away from the acidic proton H1.

The oxygen atom in **6** induces a similar but weaker contraction and depyramidalisation of the phosphorus. In this example the space required for the presence of O1 is generated

Table 3. List of geometrical parameters for the description of the structural changes of **2** when binding to different atoms.

	C–P/Å	C–P–C/°	ω/°	η/°	τ_1/°	τ_2/°	P⋯Si/Å
2[a]	1.8443(7)	102.27(13)	41(3)	63.5(13)	110.9(3)	112.1(16)	3.449(16)
4	1.800(2)	111.16(11)	51.83(11)	14.4(3)	116.52(16)	107.84(11)	3.6358(11)
5[a]	1.835(9)	105.5(15)	45.2(7)	94(7)	108.0(9)	117.7(12)	3.670(16)
6[a]	1.8161(6)	106.4(7)	39.1(17)	79(3)	111.6(12)	114.3(13)	3.545(4)

[a] Average values for equivalent parameters within the same structure. Numbers in parentheses are standard deviations of the averaged values and do not correspond to errors from the structure determination.
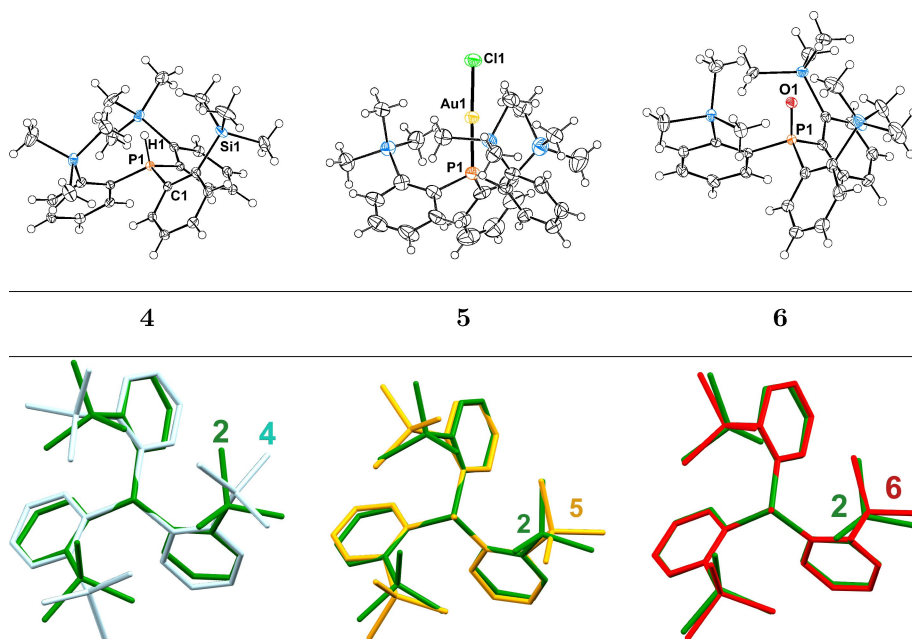
Figure 10. (Top) Displacement ellipsoid plots for the phosphine-containing residues in **4**, **5** and **6** (50 % probability). (Bottom) Overlay plots of these residues with the parent phosphine **2**.

Chemistry–A European Journal

Full Paper
doi.org/10.1002/chem.202103555

Chemistry Europe
European Chemical
Societies Publishing

by a different conformational change. While ω remains nearly the same as in plain **2** an anti-clockwise η rotation of about 15° opens the phosphorus cavity. This is accompanied by a small increase in the P⋯Si distance. Despite the significantly larger van der Waals radius of oxygen compared to hydrogen, not to mention the influence of their partial charges on their size, the phosphine cavity is not significantly larger for **6** compared to **4** (3.20 Å H⋯H above P1) and the geometry appears less strained. This may be due to the attractive interaction between the positively polarised hydrogen atoms and the negatively polarised oxygen.

In agreement with expectation, this interaction is reversed in the Au^I complex **5** and the cation requires much more space than the proton. The geometry changes are similar to those in **6** but all of the deformations are more pronounced. The P⋯Si distance is elongated the most with respect to **2**. The final cavity is enlarged to an average minimal H⋯H distance of 4.79 Å. The η torsions in this complex are suitable to position the methyl groups of each TMS moiety in a way to minimize steric repulsion among both types of methyl groups.

Although the large substituents at the now coordinated phosphorus clearly generate steric pressure, the complex does not transform to the exo_2 conformation, in contrast to the well-documented coordination behaviour of P(o-(iPr)C$_6$H$_4$)$_3$.[38] We cannot comment on possible kinetic reasons such as a high energy barrier for the necessary ring flip but simple geometry arguments confirm that a conformation with an endo TMS group can be excluded for thermodynamic reasons. We tentatively modified the structure model of the Fe(CO)$_4$ complex of P(o-(iPr)C$_6$H$_4$)$_3$ in exo_2 conformation[38] and replaced the $endo$ iPr substituent with a TMS group. For such a hypothetical exo_2 conformer, unreasonably short interatomic distances and a significant amount of steric repulsion would be unavoidable.

The AuCl complex allows to quantify the steric demand of the ligand in a coordination compound. The cone angle θ was originally conceived for a metal–P distance normalised to 2.28 Å. When the positional coordinates of the Au^I cation are modified to match this distance in **5**, a cone angle of $\theta = 250°$ is calculated.[51] When compared to popular and commercially available phosphines which are generally considered as sterically demanding such as PCy$_3$ ($\theta = 176°$) and P(o-Tol)$_3$ ($\theta = 190°$), it turns out that our ligand possesses quite a large cone angle that is matched only by ligands such as BrettPhos ($\theta = 251°$).[50] Interestingly the buried volume[26] V_{Bur} affords an exceptionally large value of 66.1%. J. Jover and J. Cirera found a linear correlation between the burried volume and the cone angle. V_{Bur} for **5** is larger by 13% than the predicted value based on the linear regression by J. Jover. The distribution of steric bulk is as expected C_3 symmetric (Figure 11) and displays areas of larger steric bulk corresponding to the τ_1 methyl groups and lower steric encumbrance associated with the τ_2 methyl groups.
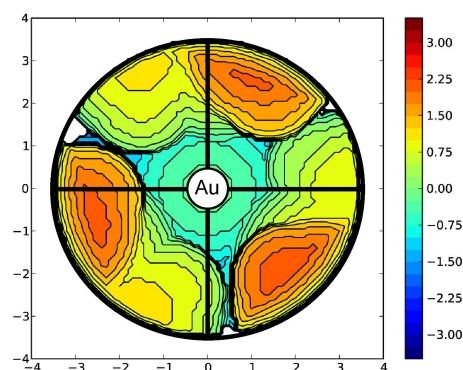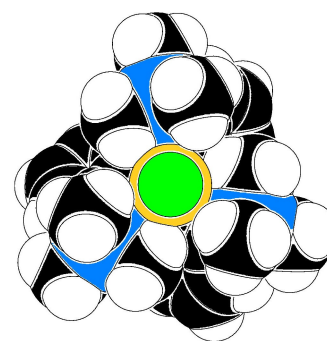
Figure 11. Space filling model of **5** and steric map[28] computed with SambVca 2.1 using default parameters.[29]

Electrochemistry

The immediate precipitation of Au^0 during the room temperature synthesis of **5** led us to the conclusion that the ligand may reduce Au^I while being oxidised itself. This is a behaviour observed for the reaction of Ag^I salts with sterically overcrowded phosphines like P(Mes)$_3$ whereas there is no reaction of **2** with Ag^I.[32] This encouraged us to investigate the electrochemical properties of **2** and compare them to two well-known phosphines: P(Mes)$_3$ is known to be reversibly oxidisable to a relatively stable radical cation, and PPh$_3$ represents the simplest example of a sterically unprotected phosphine. All electrochemical potentials are referenced to the potential of the Fc$^+$/Fc redox pair and the voltammograms are shown in Figure 12.

In agreement with several literature reports, we observed the irreversible oxidation of PPh$_3$ at 0.92 V.[53,54] Our phosphine **2** oxidises at a slightly lower potential of 0.83 V. Its oxidation is chemically reversible with $E_{1/2} = 0.78$ V, $\Delta E_p = 109$ mV and approximately equal peak currents during oxidation and reduction. This suggests that the emerging radical cation at the phosphorus is protected by the surrounding steric bulk (see more details in the Supporting Information).

The oxidation of P(Mes)$_3$ in comparison is chemically reversible as well but at a much lower $E_{1/2}$ of 0.19 V with $\Delta E_p = 77$ mV. Bullock et al. described the same trend in a series of compounds of the composition PPh$_{3-n}$(dipp)$_n$ (dipp = 2,6-diisopropylphenyl). A higher number of dipp substituents leads to more pronounced flattening of the phosphine and a lower oxidation potential. They attributed this to an increase in 3p

Chemistry–A European Journal

Full Paper
doi.org/10.1002/chem.202103555

**Chemistry
Europe**
European Chemical
Societies Publishing
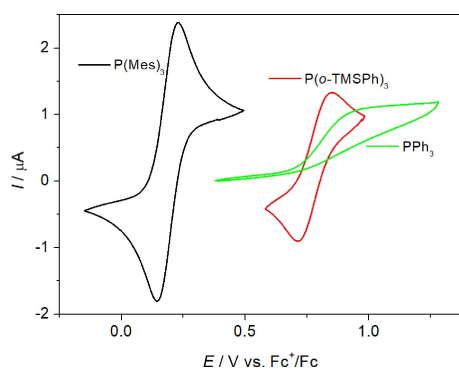
Figure 12. Comparison of the cyclic voltammograms of P(Mes)$_3$, P(o-TMSC$_6$H$_4$)$_3$ (2) and PPh3 (1 mM each) at a scan rate of 100mVs-1 at a 1 mm Pt disk electrode in CH$_2$Cl$_2$ (0.1 M NBu$_4$PF$_6$). The internal standard Ferrocene was added afterwards and all potentials are referenced to the Fc+/Fc redox couple.

character and energy of the HOMO.[54] While this explains the large difference in oxidation potentials between P(Mes)$_3$ and **2** it does not explain the lower potential of **2** compared to PPh$_3$ as they are quite similar with respect to geometry. However, the oxidation potential is also sensitive to the electronic influence of the substituents.[55] Electron donating substituents will also raise the HOMO energy and basicity of the phosphine and lower the oxidation potential.[56] This matches the electron donating effect of the TMS groups which lowers the potential slightly with respect to PPh$_3$.[57,58]

Apart from the potential itself the peak-to-peak separation of **2** (ΔE_p) is also slightly larger in **2** compared to P(Mes)$_3$. This may have a geometrical origin. Upon single electron oxidation a flattening of the phosphine geometry was predicted by theory and has been observed in single crystal diffraction.[32] The TMS groups will naturally resist a flattening of the phosphine which may cause the increase in ΔE_p.

The higher potential of **2** compared to P(Mes)$_3$ may also explain why it is not oxidised by Ag^I salts. We tried to use other strong chemical oxidants like chloranil and different Ce^{IV} salts but none of them reacted with **2** whereas they do react with PPh$_3$. Further investigation of this behaviour might be achieved by electrolytical oxidation and subsequent investigation with EPR spectroscopy, but unfortunately the required equipment is not available to us.

Catalysis

A large steric bulk around an Au^I centre can induce regioselectivity in catalytic transformations.[59–65] Meanwhile it can prevent substrate coordination and lower the catalytic activity but at the same time stabilise the catalyst against the formation of Au^0.

To test these hypotheses we abstracted the chlorido ligand from **5**, used the resulting cationic complex in the catalytic hydrolysis of 1-phenyl-1-propyne and compared its activity to that of [Au(PPh$_3$)]$^+$. The reaction conditions lead to the

Table 4. Yields by NMR Y, selectivities S and turnover numbers TON in the catalytic hydrolysis of 1-phenyl-1-propyne with our ligand **2** and PPh$_3$.

P(o-TMSC$_6$H$_4$)$_3$	t/h	Y(**7a**)/%	Y(**7b**)/%	S(**7a**)/%	TON
2	1	22	9	70	6
	3	40	17	70	11
	20	49	22	69	14
PPh$_3$	1	20	14	59	7
	3	20	14	59	7
	20	20	14	59	7

formation of Au^0 for both catalysts but [Au(PPh$_3$)]$^+$ decomposed much faster, leading to a stagnation in substrate conversion after less than 1 h. In contrast, our catalyst [Au(P(o-TMSC$_6$H$_4$)$_3$)]$^+$ remained active for more than 3 h and gave twice the total catalyst turnover before it was deactivated, thus confirming the higher stability induced by the steric bulk.

Table 4 shows that our catalyst also displays a slightly higher selectivity for **7a** over **7b**, again confirming our hypothesis. Neither the yield nor the selectivity are particularly impressive for this reaction. The results do however indicate the possibility of regioselectivity control induced by our comparably resilient catalyst.

Conclusions

The question posed in the article title – whether our sterically overcrowded phosphine is still a ligand – can clearly receive an affirmative answer. However, the scope of metal cations P(o-TMSC$_6$H$_4$)$_3$ binds to is very limited according to our findings. The coordination of Au^I requires considerable rearrangement of the ligand geometry. Nevertheless, the complex and all other reaction products of this ligand retain the *exo$_3$* conformation. The resulting complex displays catalytic activity and is able to induce regioselectivity through the steric bulk. Furthermore the oxidation potential of P(o-TMSC$_6$H$_4$)$_3$ is very similar to that of plain PPh$_3$ but the oxidation is reversible, indicating a much more stable radical cation. Future work may exploit this to investigate the electronic properties of our sterically over-crowded phosphine as a model compound for the radical cations of more simple and commercially relevant but less stable triarylphosphines.

Supporting Information

All experimental details and analytical data can be found in the Supporting Information. Furthermore it contains further details on the crystal structures. Deposition Number(s) 2112689 (for **1**), 2112695 (for **2**), 2112691 (for **3α**), 2112694 (for **3β**), 2112693 (for **4**), 2112692 (for **5**) and 2112690 (for **6**) (https://www.ccdc.cam.ac.uk/services/structures?id=doi:10.1002/chem.202103555) contain(s) the supplementary

Chem. Eur. J. **2022**, *28*, e202103555 (7 of 8)

© 2021 The Authors. Chemistry - A European Journal published by Wiley-VCH GmbH

Chemistry–A European Journal

Full Paper
doi.org/10.1002/chem.202103555

Chemistry Europe
European Chemical
Societies Publishing

Conflict of Interest

The authors declare no conflict of interest.

[1] A. W. Hofmann, *Justus Liebigs Ann. Chem.* **1857**, *103*, 357–358.
[2] J. G. J. Raj, *Rev. Inorg. Chem.* **2015**, *35*, 25–56.
[3] L. M. Pignolet, *Homogeneous Catalysis with Metal Phosphine Complexes*, Springer, New York, NY, **2013**.
[4] E. I. Musina, A. S. Balueva, A. A. Karasik, in *Organophosphorus Chem.* (Eds: L. J. Higham, D. W. Allen, J. C. Tebby), Royal Society of Chemistry, Cambridge, 37–114, **2021**.
[5] R. G. Pearson, *J. Am. Chem. Soc.* **1963**, *85*, 3533–3539.
[6] R. G. Pearson, *J. Chem. Educ.* **1968**, *45*, 643.
[7] W. W. Brennessel, J. V. G. Young, J. E. Ellis, *Angew. Chem. Int. Ed. Engl.* **2002**, *41*, 1211–1215.
[8] R. Gilbert-Wilson, L. D. Field, S. B. Colbran, M. M. Bhadbhade, *Inorg. Chem.* **2013**, *52*, 3043–3053.
[9] E. Wiebus, B. Cornils, *Chem. Ing. Tech.* **1994**, *66*, 916–923.
[10] T. Tewari, R. Kumar, A. C. Chandanshive, S. H. Chikkali, *Chem. Rec.* **2021**, *21*, 1182–1198.
[11] V. L. Budarin, P. S. Shuttleworth, J. H. Clark, R. Luque, *Curr. Org. Synth.* **2010**, *7*, 614–627.
[12] B. Schäfer, *Chem. Unserer Zeit* **2013**, *47*, 174–182.
[13] A. Biffis, P. Centomo, A. Del Zotto, M. Zecca, *Chem. Rev.* **2018**, *118*, 2249–2295.
[14] A. Yanagisawa, T. Arai, *Chem. Commun.* **2008**, 1165–1172.
[15] T. Schlatzer, R. Breinbauer, *Adv. Synth. Catal.* **2021**, *363*, 668–687.
[16] P. Dierkes, P. W. N. M. van Leeuwen, *J. Chem. Soc. Dalton Trans.* **1999**, 1519–1530.
[17] Z. L. Niemeyer, A. Milo, D. P. Hickey, M. S. Sigman, *Nat. Chem.* **2016**, *8*, 610–617.
[18] C. A. Tolman, *Chem. Rev.* **1977**, *77*, 313–348.
[19] K. Wu, A. G. Doyle, *Nat. Chem.* **2017**, *9*, 779–784.
[20] O. Diebolt, G. C. Fortman, H. Clavier, A. M. Z. Slawin, E. C. Escudero-Adán, J. Benet-Buchholz, S. P. Nolan, *Organometallics* **2011**, *30*, 1668–1676.
[21] M. an der Heiden, H. Plenio, *Chem. Commun.* **2007**, 972–974.
[22] A. Darwish, A. Lang, T. Kim, J. M. Chong, *Org. Lett.* **2008**, *10*, 861–864.
[23] A. H. Christian, Z. L. Niemeyer, M. S. Sigman, F. D. Toste, *ACS Catal.* **2017**, *7*, 3973–3978.
[24] C. A. Fleckenstein, H. Plenio, *Chem. Soc. Rev.* **2010**, *39*, 694–711.
[25] C. A. Tolman, *J. Am. Chem. Soc.* **1970**, *92*, 2956–2965.

[26] A. Poater, F. Ragone, S. Giudice, C. Costabile, R. Dorta, S. P. Nolan, L. Cavallo, *Organometallics* **2008**, *27*, 2679–2681.
[27] H. Clavier, S. P. Nolan, *Chem. Commun.* **2010**, *46*, 841–861.
[28] A. Poater, F. Ragone, R. Mariz, R. Dorta, L. Cavallo, *Chem. Eur. J.* **2010**, *16*, 14348–14353.
[29] L. Falivene, Z. Cao, A. Petta, L. Serra, A. Poater, R. Oliva, V. Scarano, L. Cavallo, *Nat. Chem.* **2019**, *11*, 872–879.
[30] S. Sasaki, M. Yoshifuji, *Curr. Org. Chem.* **2007**, *11*, 17–31.
[31] R. T. Boeré, A. M. Bond, S. Cronin, N. W. Duffy, P. Hazendonk, J. D. Masuda, K. Pollard, T. L. Roemmele, P. Tran, Y. Zhang, *New J. Chem.* **2008**, *32*, 214–231.
[32] X. Pan, X. Chen, T. Li, Y. Li, X. Wang, *J. Am. Chem. Soc.* **2013**, *135*, 3414–3417.
[33] A. V. Iltyasov, Y. M. Kargin, E. V. Nikitin, A. A. Vafina, G. V. Romanov, O. V. Parakin, A. A. Kazakova, A. N. Pudovik, *Phosphorus Sulfur Relat. Elem.* **1980**, *8*, 259–262.
[34] R. T. Boeré, Y. Zhang, *J. Organomet. Chem.* **2005**, *690*, 2651–2657.
[35] J. A. S. Howell, N. Fey, J. D. Lovatt, P. C. Yates, P. McArdle, D. Cunningham, E. Sadeh, H. E. Gottlieb, Z. Goldschmidt, M. B. Hursthouse, M. E. Light, *J. Chem. Soc. Dalton Trans.* **1999**, 3015–3028.
[36] A. S. K. Hashmi, I. Braun, M. Rudolph, F. Rominger, *Organometallics* **2012**, *31*, 644–661.
[37] J. A. S. Howell, M. G. Palin, P. McArdle, D. Cunningham, Z. Goldschmidt, H. E. Gottlieb, D. Hezroni-Langerman, *Inorg. Chem.* **1993**, *32*, 3493–3500.
[38] J. A. Howell, J. D. Lovatt, P. McArdle, D. Cunningham, E. Maimone, H. E. Gottlieb, Z. Goldschmidt, *Inorg. Chem. Commun.* **1998**, *1*, 118–120.
[39] S. Jääskeläinen, P. Suomalainen, M. Haukka, H. Riihimäki, J. T. Pursiainen, T. A. Pakkanen, *J. Organomet. Chem.* **2001**, *633*, 69–70.
[40] N. Fey, J. A. S. Howell, J. D. Lovatt, P. C. Yates, D. Cunningham, P. McArdle, H. E. Gottlieb, S. J. Coles, *Dalton Trans.* **2006**, 5464–5475.
[41] J. Bruckmann, C. Krüger, F. Lutz, *Z. Naturforsch. B* **1995**, *50*, 351–360.
[42] J. F. Blount, D. Camp, R. D. Hart, P. C. Healy, B. W. Skelton, A. H. White, *Aust. J. Chem.* **1994**, *47*, 1631.
[43] C. R. Groom, I. J. Bruno, M. P. Lightfoot, S. C. Ward, *Acta Crystallogr. Sect. B* **2016**, *72*, 171–179.
[44] A. Bondi, *J. Phys. Chem.* **1964**, *68*, 441–451.
[45] I. Dance, M. Scudder, *J. Chem. Soc. Chem. Commun.* **1995**, 1039.
[46] W. L. Koltun, Space filling atomic units and connectors for molecular models: G09b23/26, **1965**.
[47] T. Allman, R. G. Goel, *Can. J. Chem.* **1982**, *60*, 716–722.
[48] H. C. Brown, B. Kanner, *J. Am. Chem. Soc.* **1966**, *88*, 986–992.
[49] P. Schwerdtfeger, *Heteroat. Chem.* **2002**, *13*, 578–584.
[50] P. Schwerdtfeger, H. L. Hermann, H. Schmidbaur, *Inorg. Chem.* **2003**, *42*, 1334–1342.
[51] T. E. Mueller, D. M. P. Mingos, *Transition Met. Chem.* **1995**, *20*, 533–539.
[52] J. Jover, J. Cirera, *Dalton Trans.* **2019**, *48*, 15036–15048.
[53] J. A. Caram, E. J. Vasini, *Electrochim. Acta* **1994**, *39*, 2395–2400.
[54] J. P. Bullock, A. M. Bond, R. T. Boeré, T. M. Gietz, T. L. Roemmele, S. D. Seagrave, J. D. Masuda, M. Parvez, *J. Am. Chem. Soc.* **2013**, *135*, 11205–11215.
[55] M. Alcarazo, *Acc. Chem. Res.* **2016**, *49*, 1797–1805.
[56] I. Dimbarre Lao Guimarães, J. R. Garcia, K. Wohnrath, R. T. Boeré, *Eur. J. Inorg. Chem.* **2018**, *2018*, 3606–3614.
[57] J. D. Roberts, C. M. Regan, *J. Am. Chem. Soc.* **1953**, *75*, 4102–4103.
[58] C. Hansch, A. Leo, R. W. Taft, *Chem. Rev.* **1991**, *91*, 165–195.
[59] A. Fürstner, *Angew. Chem. Int. Ed. Engl.* **2018**, *57*, 4215–4233.
[60] H. Teller, M. Corbet, L. Mantilli, G. Gopakumar, *J. Am. Chem. Soc.* **2012**, *134*, 15331–15342.
[61] J. Petušková, H. Bruns, M. Alcarazo, *Angew. Chem. Int. Ed. Engl.* **2011**, *50*, 3799–3802.
[62] T. Johannsen, C. Golz, M. Alcarazo, *Angew. Chem. Int. Ed. Engl.* **2020**, *59*, 22779–22784.
[63] S. A. Shahzad, M. A. Sajid, Z. A. Khan, D. Canseco-Gonzalez, *Synth. Commun.* **2017**, *47*, 735–755.
[64] M. Mato, A. Franchino, C. Garcı A-Morales, A. M. Echavarren, *Chem. Rev.* **2021**, *121*, 8613–8684; A-Morales, A. M. Echavarren, *Chem. Rev.* **2021**, *121*, 8613–8684.
[65] J. A. Goodwin, A. Aponick, *Chem. Commun.* **2015**, *51*, 8730–8741.